# Stringlike patterns in critical polymer mixtures under steady shear flow

Erik K. Hobbie, Sanghoon Kim, and Charles C. Han
*National Institute of Standards and Technology, Gaithersburg, Maryland 20899*
(Received 26 August 1996)

Phase-contrast microscopy has been used for a quantitative study of domain deformation in diluted polymer blends undergoing spinodal decomposition in the presence of steady shear flow. Stabilized in the weak-shear limit, nearly spherical droplets of the minority phase elongate and break repeatedly as the shear rate increases, eventually giving way to stringlike patterns in the strong-shear limit. The data are interpreted with the Onuki-Taylor model of emulsionlike critical dispersions under shear. [S1063-651X(96)50512-X]

PACS number(s): 61.25.Hq, 68.10.−m, 64.75.+g

Experimental and theoretical studies of emulsions in definable fields of flow date back to Taylor [1,2], who investigated the deformation and breakup of isolated droplets under steady shear. When the viscosities of the two fluids are comparable, a spherical droplet is deformed into an ellipsoid of major axis $R_\parallel$ and minor axis $R_\perp$, which breaks into fragments when the shear rate reaches a threshold value $\dot{\gamma}_c \sim \sigma/2\eta R_0$, where $\sigma$ is the interfacial tension, $\eta$ is the shear viscosity, and $R_0$ is the radius of the undeformed droplet. An extension of this model to a binary fluid undergoing spinodal decomposition has been made by Onuki [3,4]. In the weak-shear limit ($\tau_\psi \dot{\gamma} \ll 1$, where $\tau_\psi$ is the order-parameter relaxation time) the mixture reaches a steady state in which the thermodynamic instability is ''stabilized'' by the flow [3,4]. As $\dot{\gamma}$ increases, droplets of the minority phase elongate and break as in the Taylor model [3–5]. Close to criticality in the strong-shear limit ($\tau_\psi \dot{\gamma} \gg 1$), the domains become elongated along the direction of flow [3,4], giving way to a stringlike morphology [6] with a light-scattering pattern that exhibits extreme anisotropy [6,7].

In this paper we present a quantitative study of the crossover from droplets to string patterns in a pseudobinary mixture of polystyrene (PS) and polybutadiene (PB) in a common solvent of dioctylphthalate (DOP). The average molecular weights of the components are $M_{\mathrm{PS}}=9.64\times10^4$ and $M_{\mathrm{PB}}=2.2\times10^4$, and the mixture was prepared at the close-to-critical composition of 30:70 PS:PB, with 8% weight fraction polymer in DOP. The critical temperature is $T_c \approx 68$ °C, below which the mixture phase separates into PS-rich droplets in a continuously connected PB-rich fluid. Details of the experiment are given elsewhere [8], the instrument being analogous to that described in Refs. [6] and [9]. The flow geometry is shown in Fig. 1, where the rotation axis of an ellipsoid makes an angle $\theta$ with the flow direction. At low $\dot{\gamma}$, the axis of elongation points along the principal strain direction ($\theta=\pi/4$), but as the domains elongate, $\theta$ decreases to $\sim\pi/9$ in the vicinity of the breakup [1–4].

Figures 2 and 3 show phase-contrast micrographs of the domain morphology as a function of shear rate for two different quench depths. At low $\dot{\gamma}$, droplets reach a steady state with minimal deformation. The average initial size is determined by how long the mixture is allowed to coarsen before applying shear. With increasing $\dot{\gamma}$, the droplets elongate and break repeatedly, until stringlike patterns emerge at high $\dot{\gamma}$. For the shallower quench (Fig. 3), the pattern emerges at lower $\dot{\gamma}$, with shear-induced homogenization at $\sim100$ s$^{-1}$. The asymmetric pattern is also evident in simultaneous light-scattering measurements on the same sample, which closely resemble FFT's of the real-space images [8]. We never see a percolated, bicontinuous structure as reported in Ref. [9]. Isolated droplets with extremely high aspect ratios begin to appear at around 20 s$^{-1}$ in Fig. 2 and 10 s$^{-1}$ in Fig. 3.

The Taylor model is a steady-state solution of the incompressible Navier-Stokes equation for low Reynolds number assuming an initially spherical droplet [1,2]. When the viscosities of the two phases are comparable, the aspect ratio $\zeta=R_\parallel/R_\perp$ is

$$\zeta=[(1+\tau_c\dot{\gamma})/(1-\tau_c\dot{\gamma})]+\cdots, \tag{1}$$

where

$$\tau_c = \eta R_0/\sigma \tag{2}$$

is the characteristic stress-relaxation time of the droplet. At a threshold shear rate $\dot{\gamma}_c \sim \sigma/2\eta R_0$, the stress becomes com-

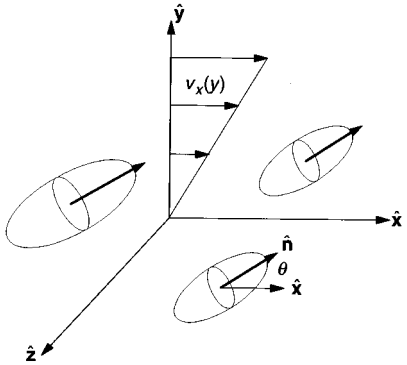


FIG. 1. The geometry of the experiment, with the optical axis of the microscope along the *y* axis, flow along the *x* axis, and vorticity in the *z* direction. The ellipsoids represent deformed droplets of the minority phase, with the tilt angle $\theta$ as shown.

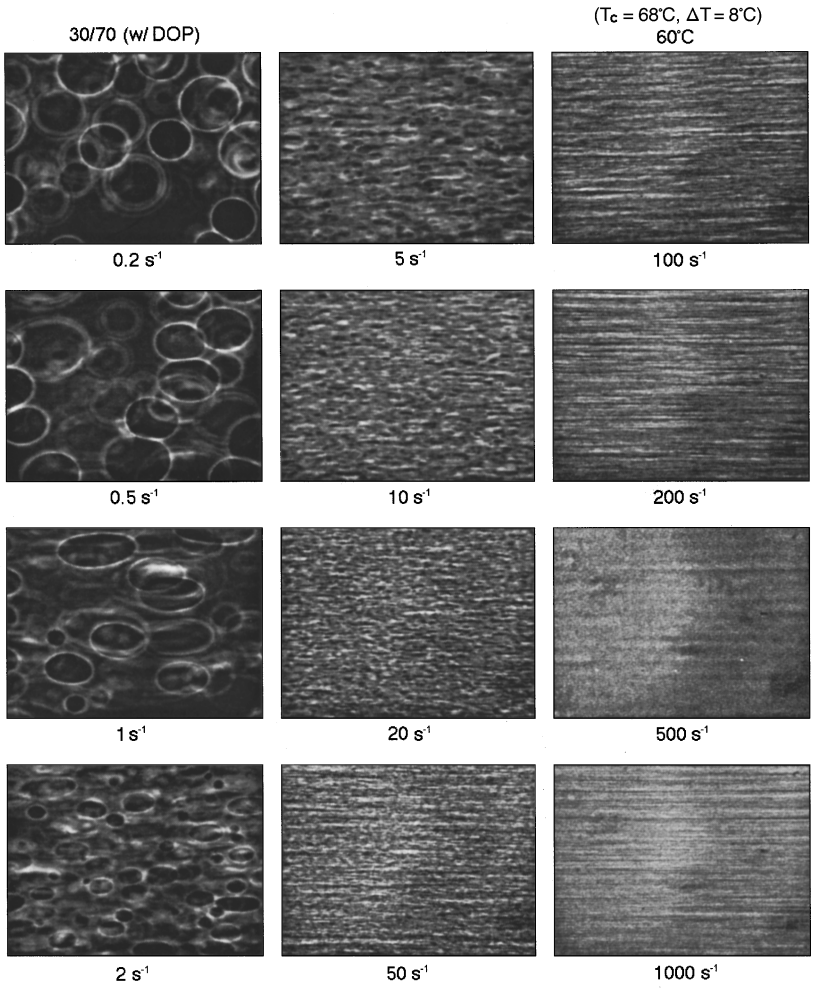


FIG. 2. Digital video micrographs of a coexisting critical mixture (30:70 PS:PB, 8% polymer in DOP, 60 °C, $T_c - T = 8$ K) under steady shear flow. The width of each micrograph is 200 $\mu$m, with the flow direction to the right, the velocity gradient out of the page, and the shear rate in 1/s. Initially spherical phase-separating droplets, stabilized by the flow in the weak-shear limit, are stretched by the shear stress until they break, and the process repeats. String patterns emerge at around 100 $s^{-1}$.

parable to the capillary pressure and the droplet breaks [1,2]. In an idealized breaking sequence, the deformed emulsion splits into two identical droplets and conservation of volume gives the recursion relations

$$R_0' = 2^{-1/3} R_0,$$
$$\tau_c' = 2^{-1/3} \tau_c, \tag{3}$$
$$\dot{\gamma}_c' = 2^{1/3} \dot{\gamma}_c,$$

which apply when a droplet of radius $R_0$ breaks into two droplets of radii $R_0'$. These relations are then applied at each consecutive breaking transition as $\dot{\gamma}$ increases, with $R_0(n) = 2^{-n/3} R_0$, $\tau_c(n) = 2^{-n/3} \tau_c$, and $\dot{\gamma}_c(n) = 2^{n/3} \dot{\gamma}_c$ after $n$ breaking transitions. For a noncritical fluid, $\zeta$ never exceeds $\zeta_{\max} \sim 2$–$3$.

An extension of the above arguments to a phase-separating critical mixture gives essentially the same result in the weak-shear limit, but ''critical'' effects become important in the strong-shear limit, where the flow leads to a shift in the critical temperature [3,4]. The surface tension in a critical fluid is $\sigma \sim (0.1) k_B T / \xi^2$, where $\xi$ is the thermal correlation length [10]. To leading order in $\varepsilon = 4 - d$ ($d = 3$ is the spatial dimension), the theory of Onuki and Kawasaki [11] predicts that the shear-induced shift in $T_c$ changes the surface tension to

$$\sigma(\dot{\gamma}) \approx \sigma_0 \{1 - A(\tau_\psi \dot{\gamma})^{1/3\nu}\}^{2\nu}, \tag{4}$$

where $\sigma_0$ is the $\dot{\gamma} \to 0$ surface tension, $A$ is an amplitude of $O(\varepsilon)$, and $\nu$ is the critical exponent associated with $\xi$. Shear-induced mixing thus leads to a reduction of $\sigma$, which implies that

$$\tau_c(\dot{\gamma}) \approx \tau_c(0) \{1 - A(\tau_\psi \dot{\gamma})^{1/3\nu}\}^{-2\nu}, \tag{5}$$

where $\tau_c(0) = \eta R_0 / \sigma_0$ is the weak-shear response time. In the crossover regime, $\tau_c(\dot{\gamma})$ increases gradually and $\zeta$ becomes slightly larger at each successive breaking transition. At a sufficiently high shear rate, $\tau_c(\dot{\gamma})$ suddenly becomes quite large, Eq. (1) blows up, and the pattern becomes string-like.

The initial structure is coarse with well-defined interfaces. Fluorescence studies [12] suggest that shear-induced mixing

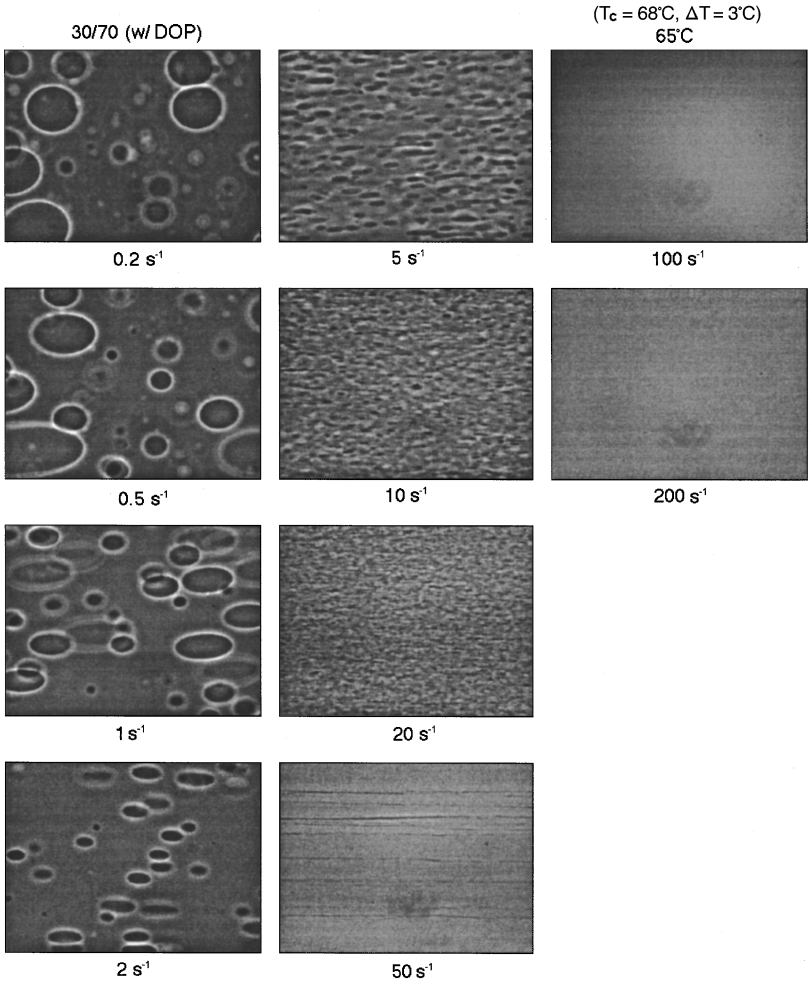


FIG. 3. Digital video micrographs similar to those shown in Fig. 2, but at a slightly higher temperature ($T$=65°C, $T_c-T$=3 K), with a stringlike pattern emerging at a lower shear rate ($\sim$50 $s^{-1}$). At higher shear rates the width of the droplet becomes comparable to the thermal correlation length $\xi$, and the mixture becomes homogeneous.

begins below a threshold droplet size, where we can make the substitution $\tau_\psi \approx \tau_c$ in Eq. (5), so that the right-hand side assumes the approximate form [13] $\tau_c(n)/[1-(\tau_c\dot{\gamma})^{0.5}/10]$. Figure 4 shows a comparison of the data from Figs. 2 and 3 with the Onuki theory. Markers represent average aspect ratios calculated from the micrographs, and the data have been rescaled assuming $\theta \approx \pi/9$. Replacing $\tau_c$ with $\tau_c(\dot{\gamma})$ in Eqs. (1) and (2), using the initial estimate $\dot{\gamma}_c \sim 1/2\tau_c \approx 1.5-1.7\ s^{-1}$, and employing the recursion relations [Eq. (3)], we calculate $\zeta(\dot{\gamma})$ for an idealized breakup sequence. The only parameter is $\tau_c$, which is determined from a fit of the first three data points at low shear, before break-

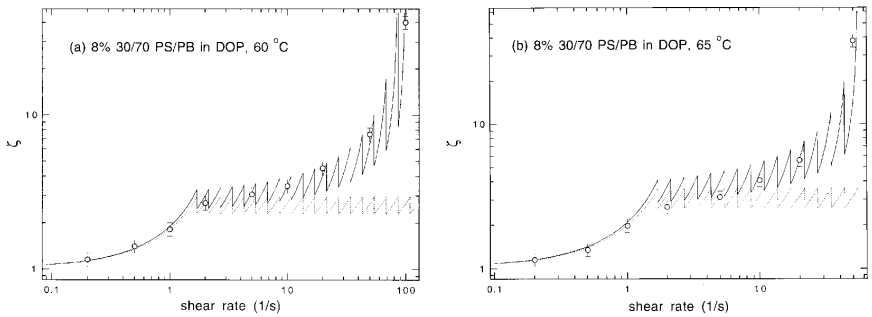


FIG. 4. Log-log plots of the string order parameter $\zeta$ as a function of shear rate for (a) the data in Fig. 2, and (b) the data in Fig. 3. The dashed lines represent an idealized breaking sequence for a noncritical droplet (Taylor), the solid lines represent an idealized breaking sequence for a critical dispersion (Onuki), and the markers represent average aspect ratios calculated from the digital micrographs, with the error bars denoting the estimated uncertainty.

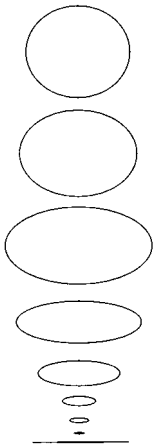

FIG. 5. Idealized breaking sequence for a droplet as a function of shear rate from the fit shown in Fig. 4(a). The elliptical shapes approximate the deformed droplet. The deformations were calculated from the Onuki theory at the shear rates (from top to bottom) 0.2, 0.5, 1, 2, 5, 10, 20, 50, and 100 $s^{-1}$, with strings emerging at $\sim 100\ s^{-1}$. Rotating each ellipse around the axis of elongation gives the ellipsoidal domain.

ing. The solid lines represent the renormalized response of Onuki, with a gradual increase in $\zeta_{\max}$ with increasing $\dot{\gamma}$, while the dashed line represents the ''mean-field'' Taylor response. The fits give $\tau_c \approx 0.29$ s for $T=60$ °C [Fig. 4(a)] and $\tau_c \approx 0.33$ s for $T=65$ °C [Fig. 4(b)]. Using $\eta \approx 0.66$ P for $T=60$ °C and $\eta \approx 0.54$ P for $T=65$ °C [14], these $\tau_c$ values yield thermal correlation lengths of $\xi \approx 7$ nm for 60 °C and 10 nm for 65 °C, which are reasonable [13]. For shear rates greater than those shown in Fig. 4, Eq. (1) blows up.

Although the breaking sequence of a droplet and its fragments is a complex process, the idealized scenario we have assumed here gives a reasonably good account of the overall behavior. Figure 5 shows how an ideal droplet evolves according to the theoretical curve shown in Fig. 4(a). The forms are elliptical cross sections with

$$R_{\perp}(\dot{\gamma}) = \zeta^{-1/3} R_n ,$$
$$R_{\parallel}(\dot{\gamma}) = \zeta^{2/3} R_n , \tag{6}$$

where $R_n = 2^{-n/3} R_0$ and $n$ is the number of breaking transitions that have occurred up to the shear rate of interest. The shapes are calculated to scale for $T=60$ °C, so the aspect ratios and relative sizes can be compared with the micrographs in Fig. 2. Stringlike behavior emerges at $\sim 100\ s^{-1}$. Note that the initial droplet distribution is polydisperse and, since the shear rate at which a droplet first breaks depends on $R_0$, the domains first break at different shear rates. On average, however, the agreement between Fig. 5 and Fig. 2 is quite good.

In conclusion, our data are consistent with the mode-coupling–renormalization-group theory of critical polymer dispersions under steady shear flow. The string patterns arise from the softening of the surface tension with shear, which in turn is linked to shear-induced homogenization. The success of this theory in such a broad class of close-to-critical mixtures, including low-molecular-weight blends, diluted blends, and small-molecule binary fluids [13,15], is truly remarkable, and speaks to the concept of universality in critical phenomena.


[1] G. I. Taylor, Proc. R. Soc. London Ser. A **138,** 41 (1932); **146,** 501 (1934).

[2] J. M. Rallison, J. Fluid Mech. **209,** 465 (1981); Annu. Rev. Fluid Mech. **16**, 45 (1984).

[3] A. Onuki, Phys. Rev. A **34,** R3528 (1986); Physica **140A,** 204 (1986); Int. J. Thermophys. **10,** 293 (1989).

[4] A. Onuki, Phys. Rev. A **35,** 5149 (1987).

[5] W. I. Goldburg and K. Y. Min, Physica **204A,** 31 (1991); T. Hashimoto, T. Takebe, and K. Fujioka, in *Dynamics and Patterns in Complex Fluids*, edited by A. Onuki and K. Kawasaki (Springer, Berlin, 1990), p. 86.

[6] T. Hashimoto, K. Matsuzaka, E. Moses, and A. Onuki , Phys. Rev. Lett. **74,** 126 (1995).

[7] T. Baumberger, F. Perot, and D. Beysens, Physica **174A,** 31 (1991);K. Fukuhara, K. Hamano, N. Kuwahara, J. V. Sengers, and A. H. Krall, Phys. Lett. A **176,** 344 (1993).

[8] S. Kim and C. C. Han, Rev. Sci. Instrum. (to be published).

[9] E. Moses, T. Kume, and T. Hashimoto, Phys. Rev. Lett. **72**, 2037 (1994).

[10] M. R. Moldover, Phys. Rev. A **31,** 1022 (1985).

[11] A. Onuki and K. Kawasaki, Ann. Phys. (N.Y.) **121,** 456 (1979); Prog. Theor. Phys. Suppl. **64,** 436 (1978); A. Onuki, K. Yamazaki, and K. Kawasaki, Ann. Phys. Suppl. (N.Y.) **131**, 217 (1981).

[12] J. Yu, S. Kim, and C. C. Han (unpublished).

[13] E. K. Hobbie, A. I. Nakatani, H. Yajima, J. F. Douglas, and C. C. Han, Phys. Rev. E **53,** R4322 (1996); E. K. Hobbie, D. W. Hair, A. I. Nakatani, and C. C. Han, Phys. Rev. Lett. **69,** 1951 (1992).

[14] H. Yajima, D. W. Hair, A. I. Nakatani, J. F. Douglas, and C. C. Han, Phys. Rev. B **47,** 12 228 (1993).

[15] D. Beysens, M. Gbadamassi, and L. Boyer, Phys. Rev. Lett. **43,** 1253 (1979); D. Beysens, M. Gbadamassi, and B. Moncef-Bouanz, Phys. Rev. A **28,** 2491 (1983).